Thermal Neutron Scattering Cross Section Measurements of Light and Heavy Water

G. Li[1], G. Bentoumi[1], Z. Tun[2], L. Li[1] and B. Sur[1]

[1] Nuclear Science Division, Atomic Energy of Canada Limited, Chalk River, Ontario, K0J1J0 Canada

(Corresponding author: E-mail: lig@aecl.ca)

[2] Canadian Neutron Beam Centre, National Research Council Canada, Chalk River, Ontario, K0J1J0 Canada

Abstract

Thermal neutron scattering cross section measurements of light (H_2O) and heavy water (D_2O) under ambient conditions were performed using a triple-axis spectrometer at the NRU reactor. The total cross section σ, as well as single ($d\sigma/d\Omega$) and double differential ($d^2\sigma/d\Omega dE$) cross sections were measured. Incident neutron energies from 15 meV to 50 meV, and scattering angles from 10° to 110° were covered. The experimental techniques and the data analysis method to obtain the absolute cross sections will be discussed and the resulting cross sections compared with the Evaluated Nuclear Data File (ENDF).

1. Introduction

The conceptual Canadian GEN-IV pressure-tube Super-Critical Water Reactor (SCWR) [1], utilizes light water coolant in the thermodynamically supercritical state with pressure at approximately 25 MPa and temperature ranging from 350 ℃ (inlet) to 650 ℃ (outlet), and heavy water moderator at relatively low pressure and temperature. The neutron distribution inside the reactor core could be obtained as the solution to the Boltzmann transport equation [2] provided there is adequate knowledge of the laws that govern the neutron interactions with surrounding materials. The coolant and moderator play the most important role in the neutron transport process, especially for neutrons in the thermal energy range. Therefore high accuracy nuclear cross section data are of great importance for the neutronic transport calculations.

At high neutron energies, the cross section is calculated by assuming that nuclei of the propagating medium are isolated particles initially at rest. Since the binding energy of the nuclei to the respective molecule or crystal lattice is much smaller than the initial neutron kinetic energy, the binding energy can be neglected. The out-going neutron's direction and energy can be derived from the laws of classical mechanics, approximating matter as a mixture of stand-alone free nuclei [3]. At neutron energies less than ~1 eV, however, it is necessary to take into account the nuclei initial energy (function of the temperature of the medium) and the effects of molecular binding. Under thermodynamically supercritical conditions, the experimental data for scattering with water are very rare, and their reliability is questionable. Currently, neutron transport simulations involving supercritical water assume that the hydrogen nucleus is unbounded, an approximation known as the "free gas model". New experimental data are undoubtedly required

to test the range of validity of this versus competing models.

The majority of the work on thermal neutron scattering was performed last century in the fifties and sixties. Since then no new measurements have been done to re-evaluate neutron cross sections. As the first step towards the cross section measurements of water in the thermodynamically supercritical state, we have performed cross-section measurements under ambient conditions. The objectives of these measurements are to reproduce the existing cross section data, analyze uncertainties and systematic effects, and re-establish the technology of inelastic neutron scattering cross section measurement for the liquids at the NRU reactor.

2. Experimental Setup

The experiment was carried out at the neutron scattering facilities of AECL Chalk River Laboratories' NRU reactor using the C5 triple axis spectrometer. The schematic layout of the instrument configuration is shown in Fig. 1. The three axes refer to the axis of the monochromator, the sample and the analyzer. The angular settings for all axes are accurate to within ±0.01°. A detailed description of the C5 spectrometer can be found in Ref. [4].

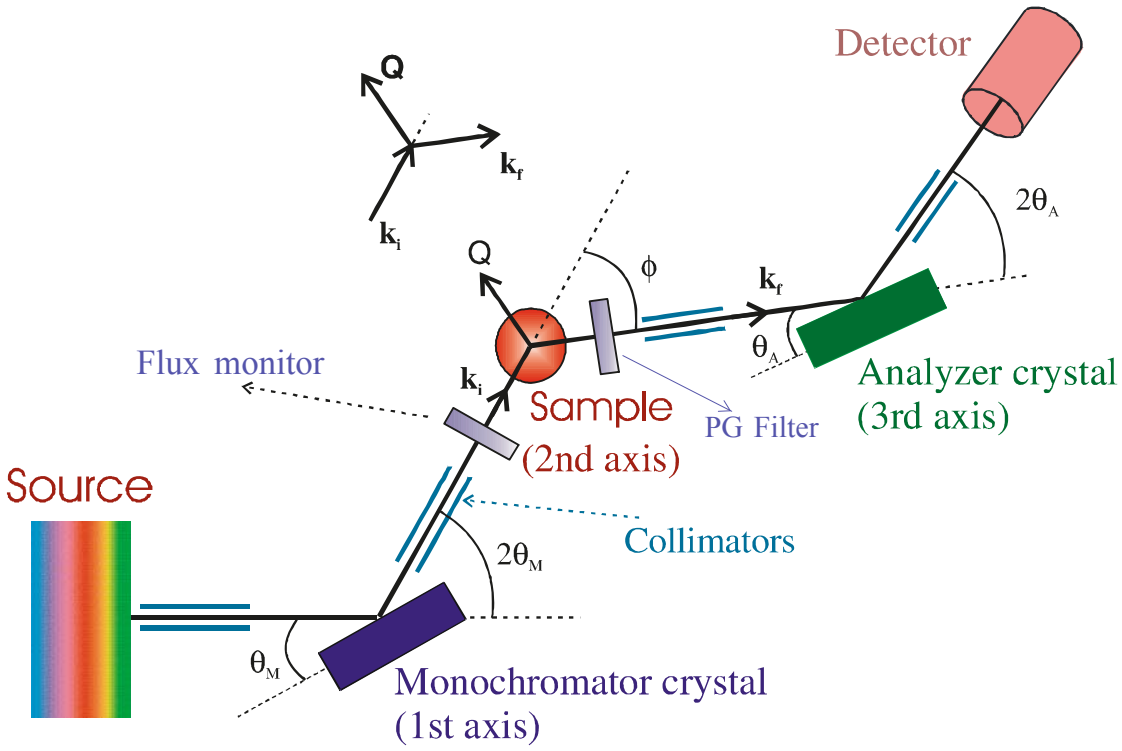

Figure. 1: Schematic drawing of the triple-axis spectrometer. The monochromator crystal at the first axis selects neutrons with a specific energy, providing a monochromatic beam. The analyzer crystal at the third axis defines the final energy. Figure is taken from [5] and modified to show the actual set up.

The incoming beam energy is determined by the Bragg angle of the [111] plane of the silicon monochromator crystal. Because of the absence of planes with half d-spacing for [111] planes in silicon, the lowest higher order contribution in the neutron beam has wavelength $\lambda/3$, or 9 times higher in energy, and is negligible for most energies used in this experiment. For this proof-of-principle experiment, a vertically focusing monochromator was selected to maximize the beam intensity.

The incident beam passed through a beam flux monitor, a ^{235}U fission ion chamber operated in pulse mode. The detection efficiency of that monitor is on the order of 10^{-4}, and is inversely proportional to the neutron velocity throughout the energy range of interest.

The water sample was held between two pure silicon plates of 1 mm thick and 10 cm in diameter, sealed with a rubber O-ring. The silicon plates are virtually transparent to neutrons. The thickness of the water can be adjusted by using O-rings of different thicknesses and by compressing the O-ring. The light water sample of thickness 0.25 mm, and heavy water sample of thickness 2.92 mm have been used for cross-section measurements. With these thicknesses, the neutron beam has about 90% transmission. The thickness of the sample is a trade-off between gaining signal intensity and avoiding multiple scattering.

The scattered neutron energy was defined by Bragg reflection from the pyrolytic graphite (PG) analyzer crystal. The scattered neutrons from the analyzer were detected using a single wire ^{3}He detector, which has detection efficiency >95% at all energies of interest.

3. Experimental procedure and results

3.1 Total cross section σ

Neutron total cross sections were measured for heavy water with beam energies from 12 meV to 50 meV. Within this energy region, there is a known discrepancy between the evaluated total cross section and previous data [6]. The total cross section was determined by measuring the transmission of neutrons passing through the sample. The transmission is defined as the fraction of incident neutrons passing through the sample compared to that without the sample. In the total cross section measurement, the triple-axis spectrometer was operated in the single-axis mode, namely, the angles at the sample and analyzer axis were set at 180°, and the analyzer was removed so the transmitted neutron beam was directly incident on the ^{3}He detector. In order to avoid saturating the detector, the beam was limited by two pin holes located before and after the sample.

The total cross section can be calculated from the transmission by Eq. (1)

$$T = \exp(-\sigma\rho_N t) \qquad (1)$$

in which T is the fractional transmission, ρ_N is the volume density of the sample and t is the sample thickness. The measured cross sections are shown in Fig. 2, along with previously published data [7] and the line shape of the total cross section evaluated at Institute for Nuclear Technology and Energy Systems (IKE) [6]. While there is general agreement in the magnitudes of the current and previous total cross-section measurements, significant discrepancies are observed at several neutron energies. Further investigation revealed that these discrepancies were most likely caused by the focusing monochromater used in this set of experiments and the resulting energy dependent incident beam geometry. Depending on the wavelength, the focused incident beam was found to diverge after the first pin hole and the divergent neutrons, which should not be detected, could be scattered by the sample and accidently pass through the second pin-hole, resulting in an apparently higher transmission and consequently lower apparent total cross-section.

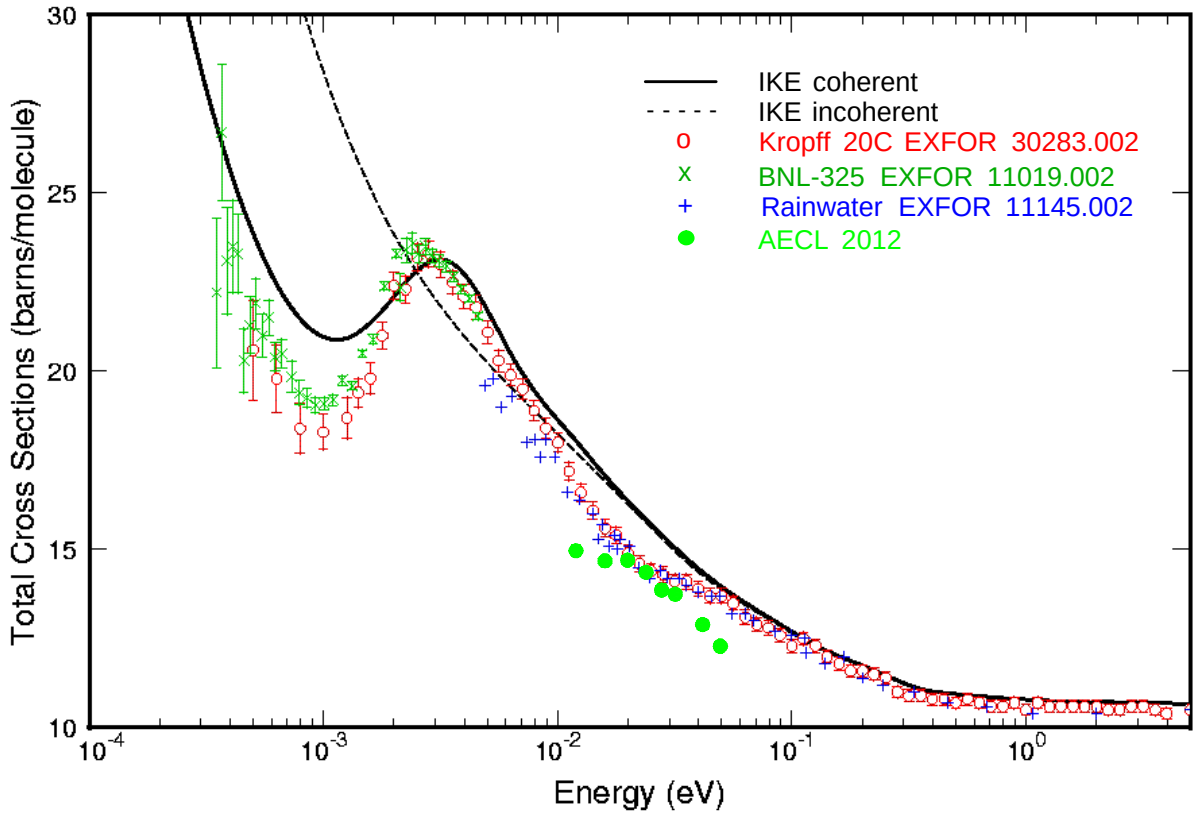

Figure. 2: Total scattering cross section of D_2O. The solid and dashed lines are the IKE evaluations [6], the green circles are the data from this experiment, and other data points are from Ref. [7]. The figure of previous data and IKE evaluations are from [6].

3.2 Single differential cross section $d\sigma / d\Omega$

The single differential cross sections for light and heavy water were measured at beam energies of

14.56 and 41.44 meV and scattered neutron angles scanned from 10° to 110°, in 5° steps. Since scattered neutrons of all energies should be detected in the $d\sigma/d\Omega$ measurement, the triple-axis spectrometer was operated in the double-axis mode, namely, the third axis in Fig. 1 was fixed at 180° and the ^{3}He detector was directly illuminated by the neutrons scattered from the sample. In this mode, the analyzer was set perpendicular to the neutron direction. Therefore only a very few neutrons, which satisfied Bragg's law, were reflected by the analyzer while the majority were transmitted to the detector.

The background was measured by removing water while the sample holder was left in place. Except for a few isolated points caused by accidental Bragg scattering from the silicon windows, the majority of the background was from the air but not the sample holder. The background was subtracted point-by-point from the raw data. In fact, the present of water in the neutron beam will change the background; therefore the true background is slightly different from the measured background.

By definition, the detected count-rate, C, in the $d\sigma/d\Omega$ measurement is

$$C = \frac{d\sigma}{d\Omega} I \cdot n\Delta\Omega \qquad (2)$$

in which I is the beam intensity, n is the areal density of the target material, and $\Delta\Omega$ is the detector acceptance angle. Experimentally, the beam intensity I and the detector acceptance angle $\Delta\Omega$ are usually difficult to establish. These factors can be accounted for by doing a relative measurement. In the present case, the absolute cross section of water was determined relative to that of vanadium measured under the same conditions. Since vanadium is, to a very good approximation, a pure incoherent scatter, the cross section of water can be calculated as

$$\frac{d\sigma_{H_2O}}{d\Omega} = \frac{\sigma_V}{4\pi} \frac{n_V}{n_{H_2O}} \frac{C_{H_2O}}{C_V}, \qquad (3)$$

in which σ_V is the vanadium total scattering cross section, n_V and n_{H_2O} are the area density of vanadium atoms and water molecules, respectively; C_V and C_{H_2O} are the measured counts from vanadium and water, respectively. Thus the measured spectrum from water almost directly represents the single differential cross section, except for a constant normalization factor.

The preliminary result of the light water single differential cross section measurement at beam energy of 41 meV is shown in Fig. 3, along with previous published data [8]. The measurement was based on Eq.(3), with the background subtracted, and the attenuation of the neutron beam through the sample material corrected. However, effect of multiple scattering was not corrected. For a sample transmission of 90%, the multiple scattering correction was expected to be low. The counting statistics in this measurement was more then 10,000 for each data point; therefore the statistical uncertainty was negligible compared to systematic uncertainties. The quoted systematic uncertainty was mainly from the background subtraction, and from uncertainty of the sample thickness measurement. The other major uncertainty will be the angular acceptance of

the detector, which has not been included. The large errors at the lower angles are due to contamination from the main neutron beam, while at 90 and 95°, the large uncertainties are from Bragg scattering from the silicon windows used to seal the water. The measured single differential cross sections of heavy water are also generally consistent with existing data within 15%.

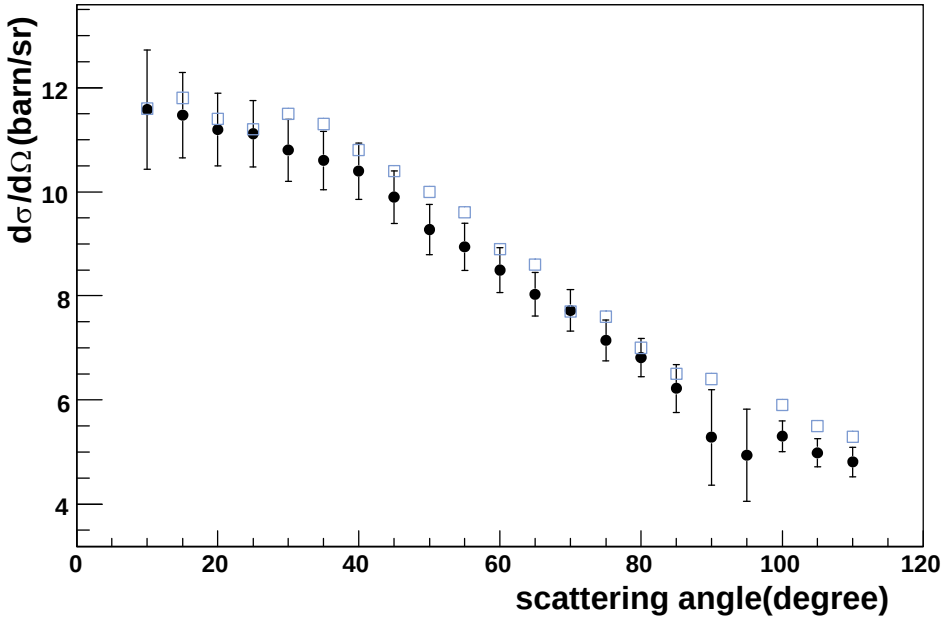

Figure. 3: Neutron scattering cross section ($d\sigma/d\Omega$) of light water with beam energy of 41 meV, in absolute unit (barn/sr). The black circless are the data of this measurement, and the open squares are the data from Beyster's measurement [8]. The error bar of the Beyster's data, which is typically 5%, is not shown.

3.3 Double differential cross section $d^2\sigma/d\Omega dE$

The neutron scattering cross section of water is usually represented by the scattering law $S(\alpha,\beta)$ [9], related to the double-differential cross-section as follows:

$$\frac{d^2\sigma_H(E_1 \to E_2,\Omega)}{d\Omega dE} = \frac{\sigma_{Hb}}{4\pi kT}\sqrt{\frac{E_2}{E_1}}e^{-\frac{\beta}{2}}S(\alpha,\beta). \qquad (4)$$

Where $S(\alpha,\beta)$ is a dimensionless function introduced by Egelstaff *et al.* [9], and α and β are defined as

$$\alpha = \frac{\Delta p^2}{2MkT} = \frac{m(E_1 + E_2 - 2\sqrt{E_1 E_2}\cos\theta)}{MkT}, \quad \beta = \frac{E_2 - E_1}{kT} \tag{5}$$

in which m is the neutron mass, M is the mass of the principal scattering atom (the proton or deuterium), θ is the scattering angle, σ_{Hb} is the bound total scattering cross section of the principal scattering atom, k is the Boltzmann constant, T is the sample temperature, E_1 and E_2 are the incident beam energy and scattered neutron energy, respectively. In the scattering law representation, the values of $S(\alpha,\beta)$ is only dependent on the neutron energy transfer and momentum transfer, which facilitates the comparison between various experiments with different beam energies.

The double differential cross section measurements were performed for scattered energies at 14.56 meV and 41.44 meV, and for scattering angles ranging from 10° to 110°. Energy transfer values up to 35 meV ($|\beta| \approx 1.4$), and neutron wave vector changes up to 7 Å^{-1} ($\alpha \approx 4$) were measured. The purpose of making two sets of measurements with scattered energies at 14.56 meV and at 41.44 meV was to produce $S(\alpha,\beta)$ under two different conditions, thereby providing a way to internally check systematic effects.

The absolute scattering cross section of water was measured relative to the vanadium scattering cross section. In the $d^2\sigma / d\Omega dE$ measurement, the measured count rate C is the convolution of the system resolution and cross section of the sample:

$$C_{(E_1 \to E_2)} = \int_0^{\Delta\Omega} d\Omega \int_{-\infty}^{+\infty} dE_B \int_{-\infty}^{+\infty} dE_A \, Beam_{(E_B)} \frac{d^2\sigma(E_1 \to E_2)}{d\Omega dE} Analyzer_{(E_A)} \times I \cdot n \tag{6}$$

in which $Beam_{(E_B)}$ and $Analyzer_{(E_A)}$ are the resolution function of the monochromator and analyzer, respectively.

The resolution of the system was measured from the scattering of a vanadium sample. Neutron scattering from vanadium is purely incoherent elastic, with the double differential cross section

$$\frac{d^2\sigma(E_1 \to E_2)}{d\Omega dE_2} = \frac{\sigma_V}{4\pi}\delta(E_1 - E_2). \tag{7}$$

The Debye-Waller factor of vanadium at room temperature can give a few percent corrections [10], and is neglected at the present experimental precision. The measurement was performed by varying the incident neutron beam energy while fixing the neutron final energy at the energy used in the water scattering measurement. The resulting spectrum can be approximated by a Gaussian distribution, as shown in Fig. 4. The overall energy resolution of the spectrometer was 1.2 and 5.6 meV at scattered neutron energy of 14.56 and 41.44 meV, respectively.

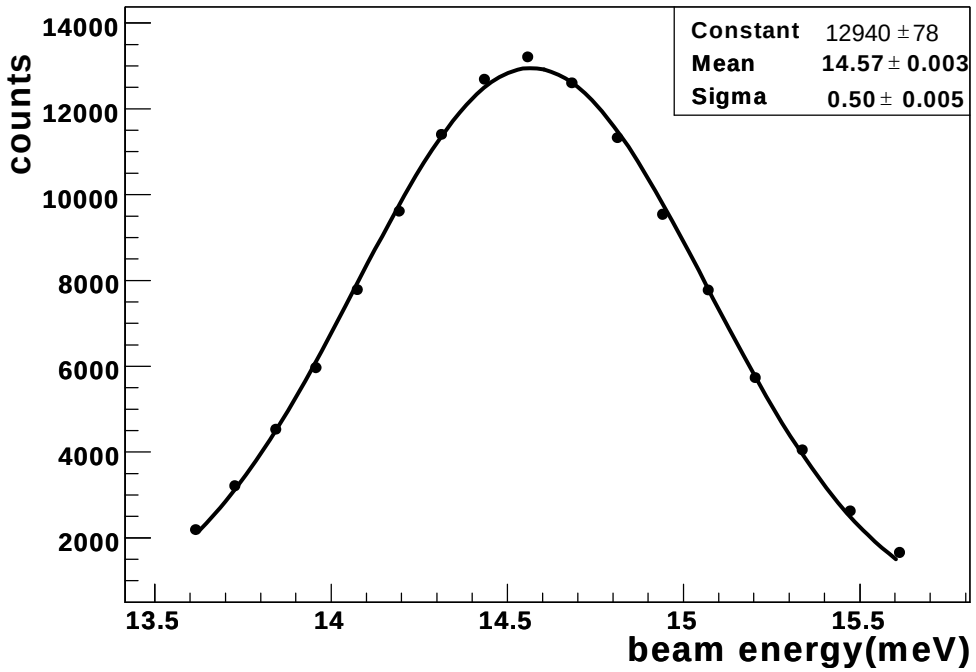

Figure. 4: Vanadium spectrum, measured by scanning the incident beam energy while keeping the analyzer set at 14.56 meV. The resolution of the spectrum represents the overall resolution of the triple-axis spectrometer. The parameters of the fitted Gaussian distribution are shown in the text box.

The full theoretical description of the normalization on the triple-axis spectrometer can be found in Ref. [11]. Combining Eqs. (6)(4)(7) and comparing the scattering from water and vanadium, the scattering law of the Hydrogen atom in the water can be expressed as [12]

$$S(\alpha,\beta)=\frac{1}{\sqrt{2\pi}}\frac{kT}{\Delta E}\frac{\sigma_V n_V C_{H(E_1\to E_2)}}{\sigma_{Hb} n_H C_{V(E_1=E_2)}} e^{\frac{\beta}{2}} \qquad (8)$$

in which $C_{H(E_1\to E_2)}$ and $C_{V(E_1=E_2)}$ are the counts from the water and vanadium scattering, respectively, both normalized to a fixed monitor count, and ΔE is the standard deviation of the fitted Gaussian function of vanadium energy spectrum as in Fig. 4. The validity of Eq. (8) assumes that:

(1) The resolution functions of the monochromater and the analyzer are Gaussian. This is generally true and can be tested by the vanadium curve as in Fig. 4.

(2) The variation of the inelastic scattering cross section is small over the system resolution. This assumption needs to be considered in a practical case as the resolution function gets broader with increasing energy, and at the quasi-elastic peak of water scattering, the broad resolution may introduce a large uncertainly.

Before using Eq. (8) to calculate the scattering law, background was subtracted, and the beam attenuation effect was corrected. Multiple scattering is another correction that needs to be considered for a high precision measurement, but was not included in the current calculation. The effect of multiple scattering has been studied for decades [13], [14] and both analytical estimates [14] and computer programs based on Monte Carlo method [15] are available to calculate the resulting corrections. A typical result of the scattering law $S(\alpha,\beta)$ for D_2O is shown in Fig. 5, with the comparison with ENDF evaluation [16]. There is significant discrepancy between the data and the ENDF evaluation, and the discrepancy is worst at the low scattering angle region (the low α region in Fig. 5). Similar discrepancies were observed for all energy transfers and with both H_2O and D_2O samples. Several reasons are suspected to cause this discrepancy. Multiple scattering becomes very serious at small scattering angles for the slab-sample geometry in transmission. A focusing beam can also introduce more counts at low scattering angles, in the sense that the actual scattering angle with a focusing beam is larger than the calculated scattering angle, which is calculated assuming a parallel beam, while at large angles the $S(\alpha,\beta)$ is usually larger, as shown in Fig. 5. The 10 mm thick vanadium plated used in the calibration introduce more uncertainties, because the geometric effects become severe at this thickness [17]. Practically similar scattering power between the vanadium and the sample is desired.

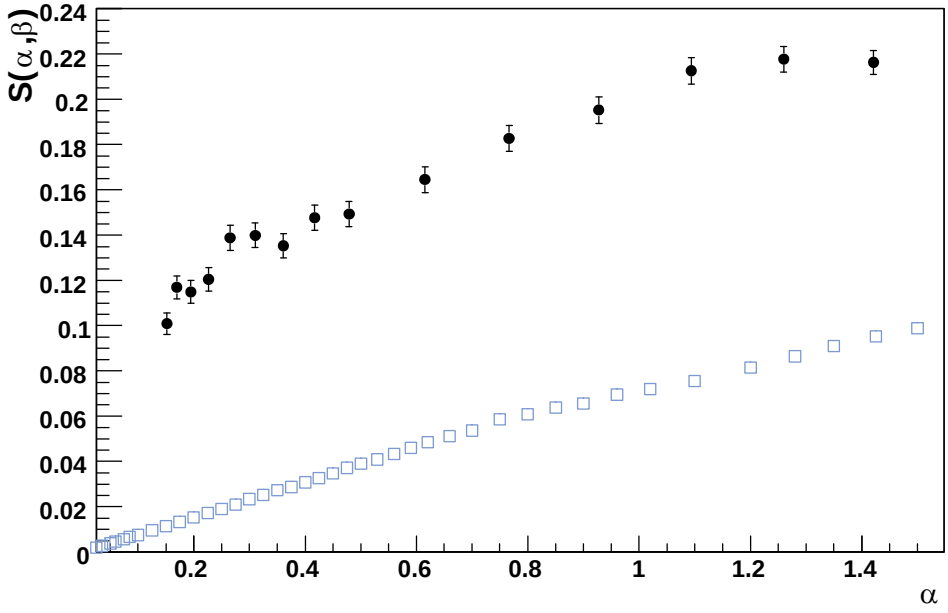

Figure. 5: The scattering law of D_2O, with energy transfer from 42.0 meV to 14.56 meV ($\beta = -1.1$), normalized by vanadium. The circles are the data and the open squares are the ENDF evaluation [16]. The uncertainties shown here are due to statistics only. The systematic uncertainties, which dominate the errors, have not been well defined therefore have not been included here.

Vanadium is usually used in the normalization of the absolute thermal neutron scattering cross section measurement, because practically speaking, it is the only natural material which has the purely incoherent elastic scatter, and its total cross section has been precisely measured. However, to normalize the absolute cross section for the inelastic scattering, a reference which has inelastic scattering property can also be used. The disadvantages of using inelastic scattering reference are: (1) the signal intensity from the inelastic scattering is much lower than from elastic scattering; (2) the cross section of the inelastic scattering is usually not measured as precisely as that of vanadium. The advantage of using an inelastic reference is that the similar properties from the reference and the sample will cancel out more systematic uncertainties.

The neutron scattering cross section with H_2O has been measured more extensively and precisely than D_2O, therefore it is legitimate to obtain the D_2O cross section relative to the H_2O measurements. From Eqs. (4) and (6), it is straightforward to express the scattering law of D_2O as

$$S_D(\alpha,\beta) = \frac{C_{D(E_1\to E_2)}}{C_{H(E_1\to E_2)}} \frac{\sigma_{Hb}}{\sigma_{Db}} \frac{n_H}{n_D} S_H(\alpha,\beta). \qquad (9)$$

The scattering law S(α,β) of heavy water in Fig. 5 was calculated using Eq. (9), and the result is shown in Fig. 6. The result is greatly improved in comparison to the cross-section obtained relative to the vanadium measurement, presumably because of the increased similarity in both the scattering properties and experimental conditions between the H_2O and D_2O measurements. Obviously the current measurement of the H_2O cross section cannot be normalized in the same way, because this would require the measurement of another inelastic scattering with better known cross section, which was not done.

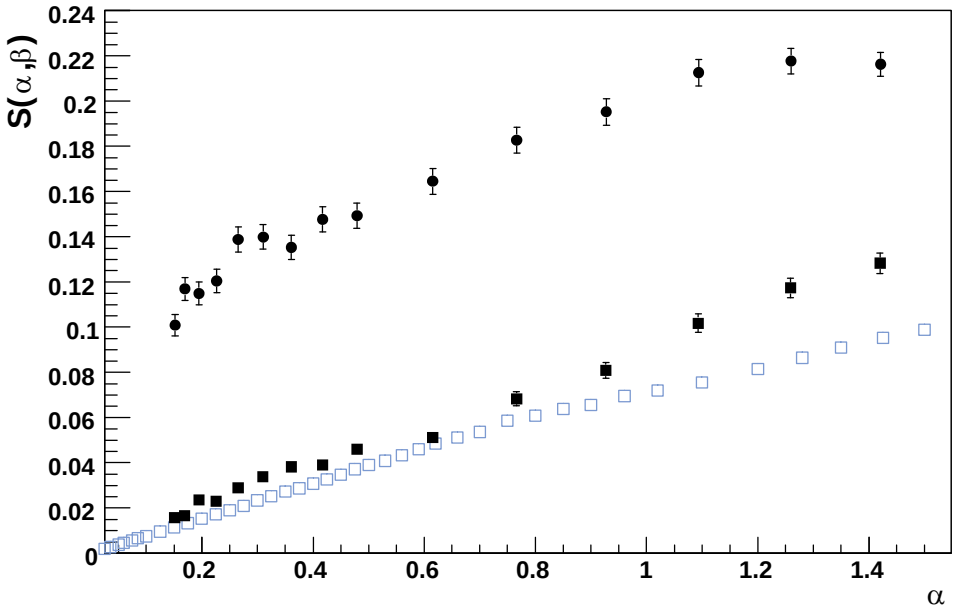

Figure. 6: An update of Fig. 5 (The scattering law of D_2O, with energy transfer from 42.0 meV to 14.56 meV), added with the $S(\alpha,\beta)$ of D_2O calculated by Eq. (9), represented by the full squares.

4. Conclusion and outlook

The thermal neutron scattering cross section measurements of light and heavy water under ambient conditions have been performed. The measured single differential cross sections ($d\sigma/d\Omega$) are generally consistent with previous published data. However, there are significant discrepancies between the measured scattering law $S(\alpha,\beta)$ and the ENDF evaluation, especially in the low momentum transfer region. Multiple scattering and the focusing property of the beam are considered to be the main causes for the discrepancies. New experiments have been scheduled to investigate these effects, by using parallel beam, and using vanadium plate with the similar scattering power as the sample. Once the measurements under ambient conditions are successfully reproduced, the experimental techniques will be almost identical to measure water under supercritical states, except for that a special cell needs to be built to hold the water under the supercritical states.

5. Acknowledgements

We acknowledge the Canadian Neutron Beam Centre staff for offering the beam time and preparing the beam line. The authors thank Zahra Yamani for valuable discussions on data analysis.

6. References

[1] L. Leung and H. Khartabil, "SCWR: OVERVIEW," in The Generation IV International Forum Symposium, Paris, France, 2009.

[2] A. Hébert, *Applied Reactor Physics*. Presses inter Polytechnique, 2009.

[3] A. Hébert, *Applied Reactor Physics*. Presses inter Polytechnique, 2009.

[4] B. N. Brockhouse, "Methods for Neutron Spectrometry," in Inelastic Scattering of Neutrons in solids and Liquids, Vienna, 1961, p. 113.

[5] Z. Yamani, Z. Tun, and D. H. Ryan, "Neutron scattering study of the classical antiferromagnet MnF2: a perfect hands-on neutron scattering teaching course," *Canadian Journal of Physics*, Vol. 88, Iss. 10, pp. 771–797, Oct. 2010.

[6] M. Mattes and J. Keinert, "Thermal Neutron Scattering Data for the Moderator Materials H2O, D2O and ZrHx in ENDF-6 Format and as ACE Library for MCNP(X) Codes," International Atomic Energy Agency, Vienna, Austria, INDC(NDS)-0470, 2005.

[7] F. Kropff, J. R. Latorre, J. R. Granada, and C. Castro Madero, "Total Neutron Cross Section of D2O at 20 °C between 0.0005 and 10 eV," EXFOR, 30283001, 1984.

[8] J. R. Beyster, "Neutron Scattering From Light Water," *Nucl. Sci. Eng.*, vol. 31, p. 254, 1968.

[9] P. A. Egelstaff, S. J. Cocking, R. Royston, and I. Thorson, "the thermal neutron scattering law for light and heavy water," in Inelastic Scattering of Neutrons in solids and Liquids, Vienna, 1961, p. 309.

[10] F. F. Freeman, B. H. Meardon, and W. G. Williams, "An experimental verification of neutron multiple scattering calculations in vanadium," *Journal of Applied Crystallography*, Vol. 11, Iss. 2, pp. 80–86, Apr. 1978.

[11] B. Dorner, "The normalization of the resolution function for inelastic neutron scattering and its application," *Acta Crystallographica Section A*, Vol. 28, Iss. 4, pp. 319–327, Jul. 1972.

[12] D. A. Kottwitz and B. R. Leonard, "The Scattering Law for Room Temperature Light Water," in Inelastic Scattering of Neutrons in solids and Liquids, 1963, Vol. I, p. 359.

[13] G. H. Vineyard, "Multiple Scattering of Neutrons," *Phys. Rev.*, Vol. 96, Iss. 1, pp. 93–98, Oct. 1954.

[14] R. Mancinelli, "Multiple neutron scattering corrections. Some general equations to do fast evaluations," *Journal of Physics: Conference Series*, Vol. 340, p. 012033, Feb. 2012.

[15] J. R. Copley, P. Verkerk, A. A. van Well, and H. Fredrikze, "Improved Monte Carlo calculation of multiple scattering effects in thermal neutron scattering experiments," *Computer Physics Communications*, Vol. 40, Iss. 2–3, pp. 337–357, Jun. 1986.

[16] "D2O scattering law," National Nuclear Data Center, 2011.

[17] P. A. Egelstaff, "14. Classical Fluids," in *Methods in Experimental Physics*, Vol. 23, Elsevier, 1987, pp. 416–417.